Porter, K. E., M. J. Lockett, and C. T. Lim, "The Effect of Liquid Chanelling on Distillation Plate Efficiency," *Trans. Inst. Chem. Engrs.*, 50, 91 (1972).
Ralston, A., and H. S. Wilf, "Mathematical Methods for Digital Computers," p. 100, Wiley, New York (1960).
Weiler, D. W., W. V. Delnicki, and B. L. England, "Flow Hydraulics of Large Diameter Trays," *Chem. Eng. Progr.*, 69(10), 67 (1973).
Yanagi, T., and B. D. Scott, "Effect of Liquid Mixing on Sieve Trays," *ibid.*, 75.
Zuiderweg, F. J., "Distillation-Science and Business," *The Chem. Eng.* 404 (1973).

Manuscript received September 16, 1974; revision received November 26 and accepted November 29, 1974.

Freeze Dehydration by Microwave Energy:

Part I. Theoretical Investigation

A general unsteady state analysis is employed to derive a mathematical model of a freeze-drying process using microwave heating. The model takes into account the variations of the transport and dielectric properties in the sample with both time and location as a function of temperature and pressure. The variations of the properties are described by functionals which have been derived from literature data and are built into the model.

The mathematical model is used to simulate the freeze drying of beef meat with microwave energy at 2450 MHz. The simulation shows that drying rates are essentially a function of the microwave power input. The model also shows that the total pressure and the partial pressure of water vapor in the vacuum chamber directly affect the sample temperature during dehydration. The simulation shows, in particular, that, an optimal microwave freeze-drying operation corresponds to an operation near corona and overheating/melting conditions.

YI HUA MA
and
PHILIPPE R. PELTRE

Department of Chemical Engineering
Worcester Polytechnic Institute
Worcester, Massachusetts 01609

SCOPE

Microwave dielectric heating has shown a great potential in accelerating freeze drying (Jackson et al., 1957; Copson, 1958). A reduction of drying time by factors of 3 to 13 has been reported when conventional (radiant) heating is replaced by microwave dielectric heating (Hoover et al., 1966). A continuous or semicontinuous process may thus be employed. Dissipation of microwave energy throughout the bulk of the material, particularly in the frozen core, accounts for the reduction of the drying time as the problem of supplying the enthalpy of sublimation by conduction from the surface is overcome.

However the lack of a systematic theoretical study of the microwave freeze drying process, as well as problems arising from applying the relatively new microwave heating technology, seem to have hampered the development of this new technique. The present work is intended to provide a mathematical simulation of the freeze drying process using microwave dielectric heating. Assuming an infinitely sharp sublimation front which retreats uniformly, a one-dimensional model is developed and used to simulate the freeze drying of beef meat with microwave energy at 2450 MHz. Effects of the microwave power input, the total pressure, and the water vapor pressure of the system and the sample thickness upon the drying process are investigated. Such a parametric study is essential for a better understanding of the freeze drying process and provides a useful tool for future process design, optimization and control.

CONCLUSIONS AND SIGNIFICANCE

Application of the mathematical model to the freeze-dehydration of beef meat at 2450 MHz shows that drying rates are essentially a function of the microwave power input. The total pressure and the partial pressure of water vapor in the vacuum directly affect the sample temperature during drying but have little effect on the drying time. Low operating vacuum chamber pressures are necessary to ensure a temperature of the frozen core as low as possible and thus allow one to use a higher microwave power input to shorten the drying time. However, pres-

Correspondence concerning this paper should be addressed to Y. H. Ma. P. R. Peltre is with the U.S. Army Natick Laboratories, Natick, Massachusetts.

sures below 50 μHg are impractical as the pressure effect becomes insignificant while the gas flow regime in the pores of the dried product becomes Knudsen diffusion. However, a lower pressure permits a higher field strength to be used without corona and thus may give a higher freeze-dryer output. The initial temperature of the sample, prior to drying, is not a significant parameter.

A reduction of the sample thickness results in a shorter drying time and a greater output of the freeze dryer as a higher microwave power input is possible without the sample being overheated or melted. The maximum freeze dryer output is thus limited by the occurrence of a corona discharge in the microwave applicator under a near overheating/melting operation.

Dehydrated food products have received a considerable amount of attention as they greatly simplify storage and conservation problems. Among various means of dehydration, the freeze-drying process is of special interest as it is most suited for heat sensitive materials such as biological and food products. Moreover, food dehydration by freeze drying provides a process which causes very little irreversible changes in foods. In freeze dehydration, the material to be dried is first deep frozen and then dehydrated by sublimation of its frozen moisture content. As the dehydration proceeds, an outer dried layer forms while the frozen core retreats. The sublimation is maintained by keeping the sublimation zone temperature below the melting point of the frozen material. The dehydration is generally conducted under vacuum although a sublimation under atmospheric conditions is physically possible (Hohner, 1970).

Microwave dielectric heating supplies energy of sublimation volumetrically and thus offers the potential of increasing the drying rate by an order of magnitude above that of conventional methods. However, the lack of a systematic theoretical study of the microwave freeze-drying process as well as problems arising from the application of the relatively new microwave heating technology seem to have hampered the development of this new technique.

Previous work in the microwave freeze-drying process concentrates mostly on experimental investigations (Jackson et al., 1957; Copson, 1958; Hoover et al., 1966; Gouigo et al., 1969; Ma and Peltre, 1975). No comprehensive theoretical analysis of this process has been reported. Previous analyses have been limited to simplified approaches using a quasi steady state assumption (Copson, 1962).

Although theoretical studies of conventional (radiant heating) freeze drying are not applicable to microwave freeze drying, it is of interest to review some of the most recent and complete studies as they emphasize the need for a general, transient analysis of the freeze drying process. It also should be pointed out that a model for microwave freeze drying could be applicable to conventional freeze drying.

These studies have generally employed the simplifying assumption of a pseudo steady state. This assumption is not applicable to microwave freeze drying because of the fast temperature transients occurring in the sample. However, this assumption is generally quite good in the radiant heating case as shown by Sandall et al. (1967). Hill and Sunderland (1971) have presented a theoretical analysis considering the simultaneous energy and mass transfer during dehydration. Although they considered the time variation of the interface temperature, they have neglected the transient behavior of temperature and concentration both in the ice-core and in the dry layer. Fox and Thompson (1972) considered the transient transport equations in the dry layer for two limiting cases: quasi steady state with heat leakage in the ice-core and transient solutions with a uniform ice-core temperature. Hohner (1970) considered the transient behavior of both mass and energy transport equations in the dry layer with a numerical technique. The reader is referred for more information to the review of King (1971).

The objective of the present work is to develop a mathematical model to describe the microwave freeze-drying process and to study the responses of the model to various freeze-drying conditions. The validity of the simulation is verified later by comparing the theoretical results with experimental data.

MATHEMATICAL MODELING

The Physical System

The material to be freeze dried is assumed to have the geometry of an infinite slab as shown in Figure 1. The left edge of the slab is insulated (or may be considered the center line of a symmetric slab) while the right edge is exposed to a vacuum at temperature T_R and concentration C_R. As the sublimation proceeds, a dry outer layer forms while the frozen core retreats. A sharp sublimation zone has been observed experimentally to separate the nearly completely dried layer and the fully hydrated and frozen core. The hypothesis of an extremely sharp sublimation zone (interface) retreating uniformly is made in this study. It seems to be a reasonable assumption (King, 1971) for the description of the freeze-drying mechanism, despite the fact that some broadening of the sublimation zone may occur, particularly near the melting point due to liquid diffusion (Bralsford, 1967).

The water vapor from the sublimation at the ice-front is removed by diffusing through the porous dry layer. At

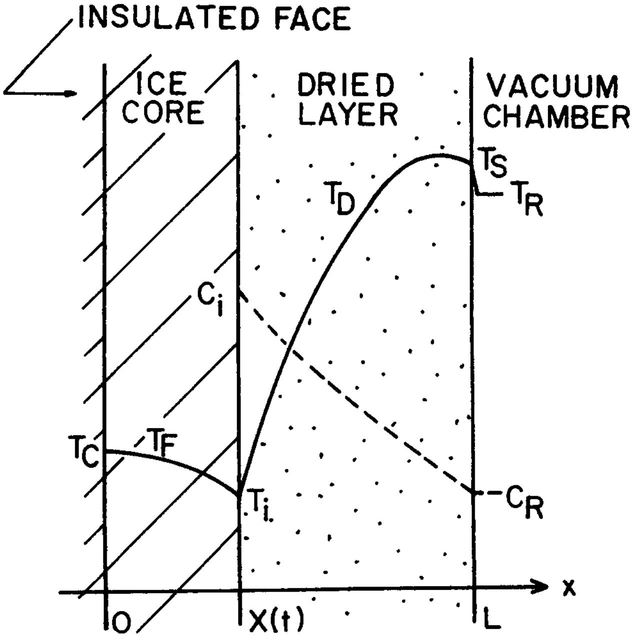

Fig. 1. Model with expected forms of the concentration and temperature profiles for the microwave freeze-drying process.

the usual operating pressure range (0.05-1 mmHg) of freeze drying the mean free path of the molecules inside the pores is of the order of magnitude of the mean pore diameter [100μ as observed by Harper (1962) for beef meat]. Thus, the flow regime corresponds to the transition region between molecular flow and slip flow. Rather complex equations have been proposed to describe gas flow in the transition region (Wakao et al., 1965). However, it is possible to describe the flow by Fick's Equation using an effective diffusivity D (Sandall et al., 1967), particularly at the lower pressure (near 0.1 mmHg) as Knudsen diffusion becomes predominant:

$$W = -D\frac{\partial C}{\partial x} \tag{1}$$

where D can be estimated by a simple two parameter model as suggested by Sandall et al. (1967).

$$D = \frac{D^0}{D^0/D_K + P} \tag{2}$$

where the pressure P is in atmosphere, D_K is the Knudsen diffusivity, and D^0 the bulk diffusivity at 1 atm. Unfortunately, a value of the Knudsen diffusivity D_K is not available for dried beef. Thus, diffusivity values for turkey meat reported by Sandall et al. (1967) were used in Equation (2) to calculate D in the theoretical study. These values are corrected to the average operation temperature expected in the dry layer (20°C) assuming that D^0 varies as $T^{1.5}$ and D_K as $T^{0.5}$. Further temperature effects on D are neglected as calculations show that maximum variations of D are less than 20% compared to a minimum 15% expected uncertainty on D. The following functional is used to describe the variations of D in the model:

$$D = 78.5/(3.4 + P) \tag{3}$$

where the pressure P is in mmHg. Use of turkey data at this stage seemed a reasonable approximation at relatively low pressures considering the rather good agreement between D value calculated by Equation (2) (using D^0 and D_K values for turkey) and that reported by Dyer and Sunderland (1966) at 1.44 torr for dried beef (see Table 1).

It should be pointed out that typical pressure variations across the dry layer (from around 4 mmHg at the ice-front for near melting operation to 0.05 mmHg at the external surface) results in a 115% variation on D as calculated by Equation (3). This variation of D with pressure is expected to have an important effect on the process as it directly affects the ice-core temperature during the drying.

It should be further pointed out that D is quite significantly affected by predrying preparation of the sample, such as freezing. The size of the pores open to the water vapor flow in the dry layer depends very much upon the rate of freezing due to the formation of ice crystals of different sizes. Thus, there is a need for comprehensive experimental D data which would account for this effect.

The necessary enthalpy of sublimation at the ice-front is supplied by the microwaves whose interaction with the dielectric medium results in a volumetric heat generation term ω. The microwave heat generation terms ω_F and ω_D are calculated from the dielectric properties of the frozen and dry beef for a given electric field strength by

$$\omega = KE^2 \tag{4a}$$

with

$$K = \pi f \epsilon_0 \epsilon''/(\epsilon'^2 + \epsilon''^2) \tag{4b}$$

assuming a uniform electric field distribution and a dominant polarization of the electric field normal to the surface of the sample as expected for the experimental setup used in this investigation (Ma and Peltre, 1974). It should be noted that a tangent polarization of the field would change (4b) to

$$K = \pi f \epsilon_0 \epsilon'' \tag{4c}$$

The attenuation effect in the dielectric is neglected. Minimum penetration depths (E reduced to $1/e$ its value at the surface) are about 3.5 cm for frozen beef (near melting). The maximum half sample thickness considered in this study is less than 1.3 cm. The dielectric properties of frozen and dry beef are very much a function of the temperature (see Figures 2 and 3) and thus are expected to vary significantly with location and time in the sample during drying. Since the dissipation coefficients K_F and K_D determine the amount of power absorbed by the product, this is a very important effect which must be taken into consideration. Dielectric data reported by Kan and Yeaton (1961) for frozen and dry beef at 3000 MHz are used to describe the variations of K_F and K_D with temperature (see Figures 2 and 3). It should be pointed out that the effect of the amount of bound (or free) unfrozen water on K_F in frozen meat is lumped into that of temperature. The effect of the amount of residual adsorbed water in the dry layer upon K_D is partially taken into account through that of temperature. However, its effect on K_D due to variations of relative humidity were not included in the calculations as dielectric data for dry beef at variable relative humidity were not available.

The heat transfer in the frozen region is assumed to be governed by conduction, while in the dry layer it is as-

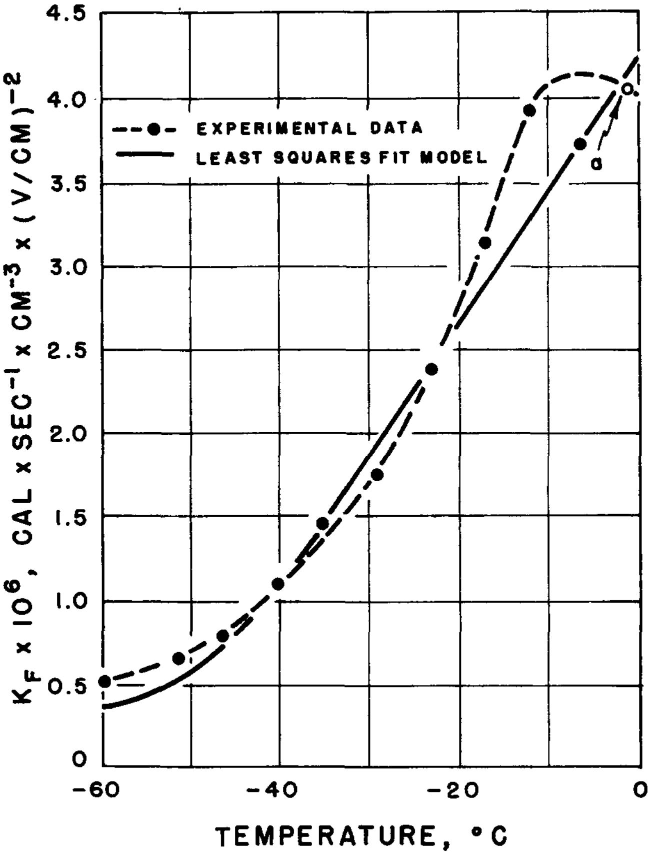

Fig. 2. Variation of K_F with temperature. Dielectric data of Kan and Yeaton (1961) for frozen beef at 3 GHz are used to calculate the dissipation coefficient K_F by

$$K_F = \pi f \epsilon_0 \epsilon''/(\epsilon_F'^2 + \epsilon_F''^2)$$

a: average among three consecutive points.

TABLE 1. REPORTED DIFFUSIVITY DATA AND COMPUTED VALUES (SUPERSCRIPTED)

Material used	T °K	D_K cm²/s	D^0 cm²/s	$D_{1.44\ torr}$ cm²/s	Tortuosity	Porosity	Literature source
Turkey breast	265	22	.09	15[c]	1.5[a]	—	Sandall et al. (1967)
	265	20	.1345	16[c]	1.0[a]	—	Sandall et al. (1967)
Beef	311	—	.045	—	4.4	.64	Harper (1962)
Beef	265	—	.037[b]	10[c]	4.4	.64	Harper (1962)
Beef	—	—	—	14	—	—	Dyer and Sunderland (1966)

[a] Computed in this investigation from the ratio D^0/D^0 free gas reported in the quoted reference, assuming a porosity of 0.64 for the dried material.
[b] Corrected at 265°K for comparison to value of Sandall et al. assuming that D^0 varies at $T^{1.5}$.
[c] Computed by Equation (2) for comparison to Dyer and Sunderland's value, assuming $D_K = 21$ cm²/s.

sumed to be governed by conduction and convection due to the flow of water vapor. The thermal conductivities of frozen k_F and dried beef k_D vary quite significantly with temperature and pressure (see Figures 4 and 5). Temperature variations in the frozen portion of the product may result in a 50 to 75% variation on k_F while pressure variations in the dry layer may induce variations of k_D as high as 75%. Thus, it is necessary to consider the variations of k_F and k_D with location and time. They are expected to have a direct effect on the actual temperature profiles in the product which are important with respect to the problems of melt back and overheating.

There is evidence that the adsorption phenomenon of the water vapor diffusing through the dry layer has little effect upon the microwave sublimation drying process. In effect, experimental freeze-drying rate curves show [see Ma and Peltre (1975), Figure 4] that the drying rate drops abruptly when the ice core disappears and drying becomes limited to the removal of residual adsorbed water. Thus, the contribution of the adsorbed water to the overall freeze-drying process can be expected to be negligible.

The Mathematical Model

A general unsteady state analysis has been used to derive a one-dimensional mathematical model of the physical system described above (Peltre, 1974). Solution of the resulting complex system of differential equations permits simulation of the microwave freeze-drying process on a digital computer. The transport phenomena involved in the process, as described above, are described by the following equations:

Mass transfer in the dry layer

$$\frac{\partial^2 C}{\partial x^2} + \frac{1}{D}\frac{\partial D}{\partial x}\frac{\partial C}{\partial x} - \frac{\sigma}{D}\frac{\partial C}{\partial t} = 0 \qquad (5)$$

Heat transfer in the dry layer

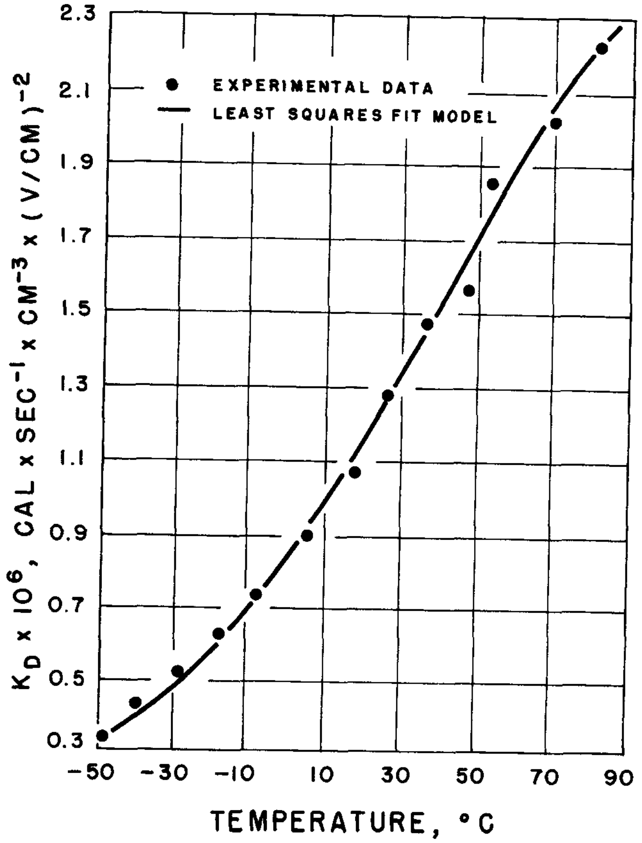

Fig. 3. Variation of K_F with temperature. Dielectric data of Kan and Yeaton (1961) for dry beef at 3 GHz are used to calculate the dissipation coefficient K_D by

$$K_D = \pi f\, \epsilon_0 \epsilon''_D/(\epsilon'_D{}^2 + \epsilon''_D{}^2)$$

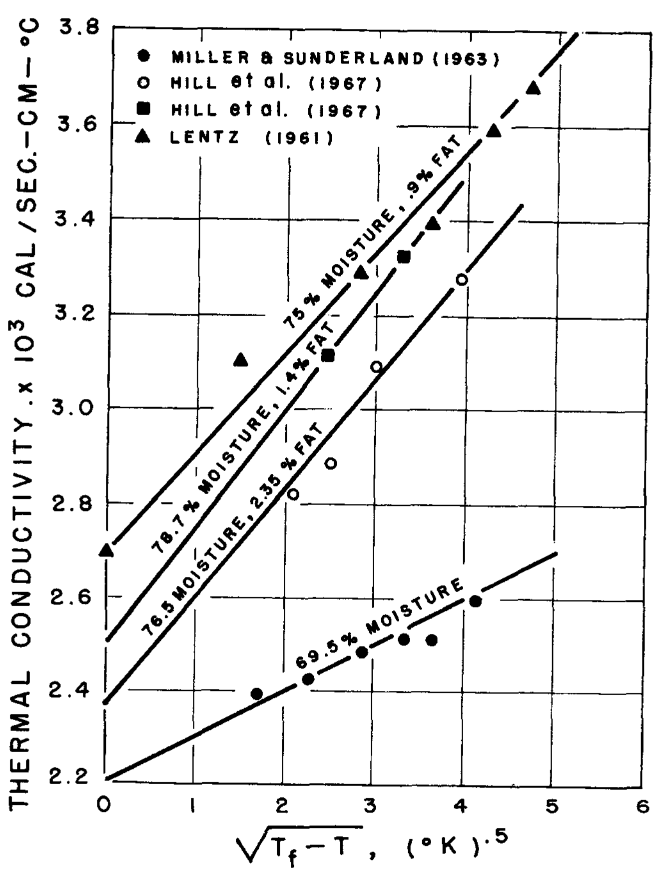

Fig. 4. Thermal conductivity of frozen beef as a function of $\sqrt{T_f - T}$ for various moisture and fat contents.

$$\frac{\partial^2 T_D}{\partial x^2} + \left(\frac{1}{k_D}\frac{\partial k_D}{\partial x} - \frac{C_{pw}W_i}{k_D}\right)\frac{\partial T_D}{\partial x} - \frac{1}{\alpha_D}\frac{\partial T_D}{\partial t} = -\frac{\omega_D}{k_D} \quad (6)$$

And in the frozen region

$$\frac{\partial^2 T_F}{\partial x^2} + \frac{1}{k_F}\frac{\partial k_F}{\partial x}\frac{\partial T_F}{\partial x} - \frac{1}{\alpha_F}\frac{\partial T_F}{\partial t} = -\frac{\omega_F}{k_F} \quad (7)$$

The water vapor from the sublimation of ice diffuses through the dry layer across a water vapor concentration gradient to the surrounding vacuum atmosphere. A vapor trap maintains a low ambient partial pressure of water vapor and acts as the mass transfer sink. This is represented mathematically by the boundary condition at the outer surface of the product:

$$C(L, t) = C_R \quad \text{for} \quad t > 0 \quad (8)$$

The necessary enthalpy of sublimation is supplied by the energy dissipated by the microwaves in the product which result in a heat flow to the sublimation front across a temperature gradient. The sublimation front acts as the heat sink which can be represented mathematically by

$$k_F\left(\frac{\partial T_F}{\partial x}\right)_i - k_D\left(\frac{\partial T_D}{\partial x}\right)_i = -W_i \Delta H_s \quad \text{for} \quad t > 0 \quad (9)$$

Finally the rate of movement of the sublimation front is related to the rate of sublimation by

$$-\rho\sigma\frac{dX}{dt} = W_i \quad (10)$$

The general procedure of solution of the partial differential equations is mainly identical to that described in an earlier publication (Ma and Peltre, 1973) with the difference that the transport and dielectric properties here are allowed to vary with both time and location. The final equations are solved numerically in the fixed boundary domain. The Crank-Nicolson method is used in conjunction with an iterative procedure. More details on the general procedure and the numerical algorithm used in the solution can be found elsewhere (Ma and Peltre, 1973; Peltre, 1974).

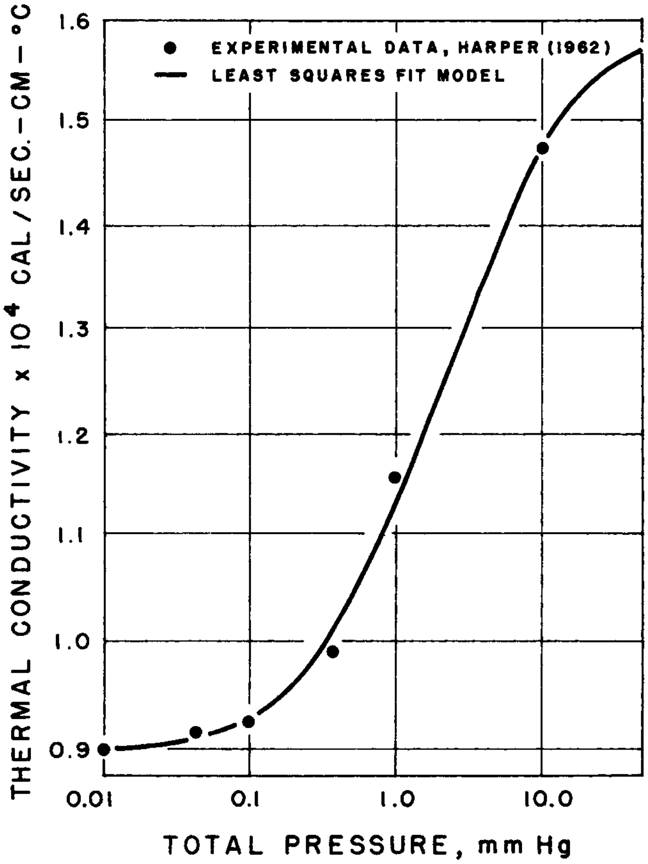

Fig. 5. Thermal conductivity of dry beef as a function of pressure.

TABLE 2. NUMERICAL VALUES OF THE CONSTANTS USED IN THE SIMULATION

Constant	Numerical value used	Origin
h	5×10^{-4} cal/cm²-s-°C	assumed
ρ	0.92 g/cm³	CRC Hdbk
ρ_D	0.32 g/cm³	measured
ρ_F	0.96 g/cm³	measured
C_{pw}	0.5 cal/g-°C	assumed
C_D	0.36 cal/g-°C	Awberry and Griffiths (1933)
C_F	0.43 cal/g-°C	Rey (1964)
ΔH_s	675 cal/g	Hohner (1970) after Threlkeld (1962)

TABLE 3. ASSUMED OPERATING CONDITIONS

E	=	125 V/cm
P_R	=	0.29 mmHg
$P_R{}^W$	=	0.075 mmHg
T_R	=	20°C
T_0	=	−15°C
L	=	1.27 cm
x_w	=	0.73
x_f	=	0.009

RESULTS AND DISCUSSION

The mathematical model has been used to simulate the freeze drying of beef meat with microwave energy at 2450 MHz. The sample is assumed to have the geometry of a one-dimensional symmetric slab with drying on both sides. Calculations were carried out in order to study the effects of the process variables and constraints of the process upon the total drying time. The numerical data for the physical properties used in the calculations are given by Equation (3), Figures 2 to 5 and Table 2. Care must be exerted to extend the present results to other practical systems as it is important to have more specific and comprehensive experimental data on the physical properties.

Typical Simulation Outcome

The operating conditions assumed in the calculations are shown in Table 3. Typically, the outcome of the simulation is similar to that which was reported and discussed in an earlier publication (Ma and Peltre, 1973). The main difference resides in the fact that the model used here allows the transport and dielectric properties to vary with both time and location in the sample as a function of temperature and pressure. In addition, the present model accounts for a 30-min. startup period during which the microwave power is still off while the vacuum is established.

The concentration profiles in the dry layer (Figure 6) exhibit a rather small curvature. In the previous study (Ma and Peltre, 1973) of the same process in which the properties were assumed uniform and constant, the concentration profiles were found to be straight lines. Thus, this small curvature may be attributed to the variation of the diffusivity with location.

Figures 7 and 8 illustrate the two drying stages described by the model. A 30-min. startup stage during which the vacuum is established with no microwave power is followed by microwave drying for the rest of the process. The endpoint is taken as the time at which the frozen core

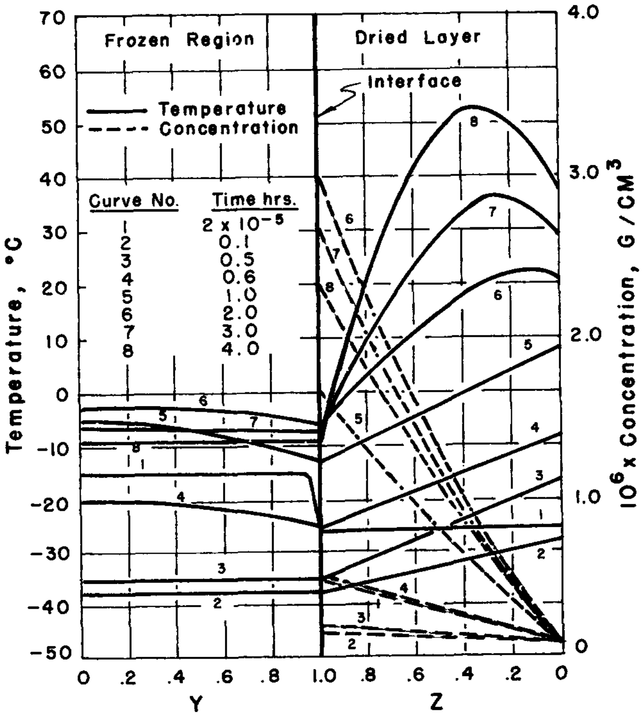

Fig. 6. Typical concentration and temperature profile for the microwave freeze-drying process

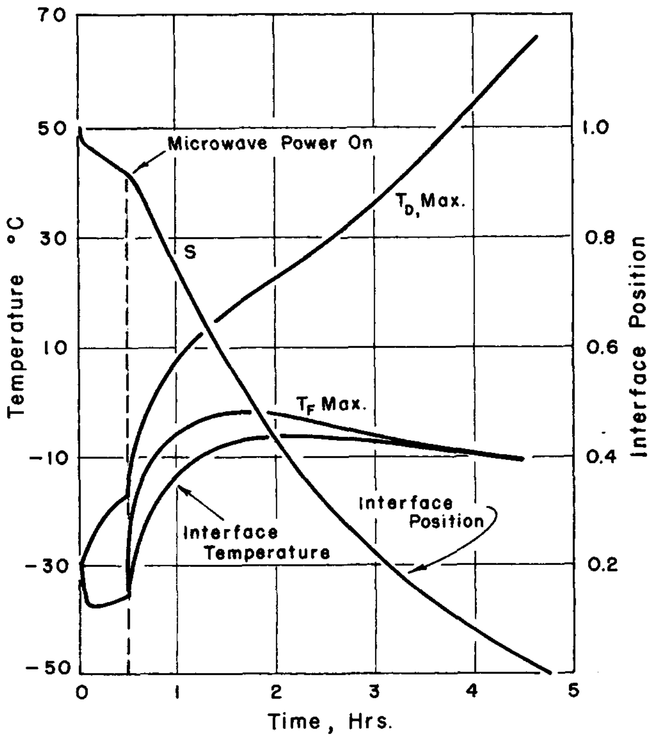

Fig. 7. Variations of the temperature and of the interface position as a function of time.

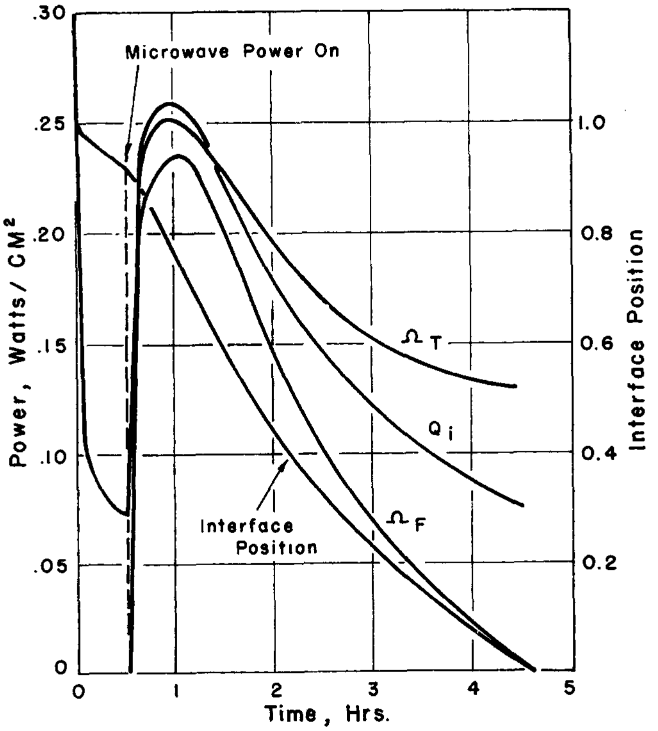

Fig. 8. Variations of the power absorbed in the sample and of the interface position as a function of time.

disappears. At time $t = 0$, as the vacuum is established, Figure 7 shows that the temperatures drop to a minimum as the ice-front temperature drops to the wet-bulb temperature of the vacuum chamber. This is illustrated in Figure 8 by the high initial rate (or power consumed by the sublimation Q_i) as the dry layer thickness is very small, which causes the fast loss in sensible heat of the frozen core.

The wet bulb temperature of the vacuum chamber, which is reached by the ice-front is different from the frost temperature in the chamber, as a small drying rate exists due to heat supplied from the surrounding atmosphere to the sample. As the thickness of the dry layer is increased due to the sublimation, the mass transfer resistance through the dry layer increases. Thus, the ice-front pressure and temperature increase. The slow decrease of the power consumed by the sublimation (supplied from the surroundings) at the interface in Figure 8 reflects the augmentation of the resistance to the heat transfer as the thickness of the dry layer increases. As the microwave power is turned on at time $t = 30$ min., the temperatures start to rise to a maximum and then decrease again as was previously observed and discussed (Ma and Peltre, 1973).

The maxima of the total microwave power absorbed Ω_T and the microwave power absorbed in the frozen region Ω_F (Figure 8) reflect the fact that the dissipation coefficient increases with the temperature in the frozen and dry regions. Ω_T and Ω_F in Figure 8 have been calculated by

$$\Omega_T = \Omega_F + \Omega_D \quad (11a)$$

$$\Omega_F(t) = \int_0^{X(t)} \omega_F(x, t)\, dx \quad (11b)$$

and similarly for Ω_D. The ω's are defined by Equation (4a). The power consumed by the phase change Q_i is related to the drying rate by $Q_i = \Delta H_s W_i$. The strong similarity of the drying rate curve with that of the power input suggests that the energy supply rate is the controlling mechanism.

Feasible Domain of Operation

The operating range for the process variables is limited to a finite feasible domain of operation—due to existing upper limits on the electric field strength and the temperature maxima in the product being dried. These physical constraints can be expressed mathematically by

$$E < E_B(P_R) \qquad (12a)$$

$$T_{F,\max}(E, P_R, P_R^W, L) < T_{\text{melting}} \text{ (around } -1.5°\text{C)} \qquad (12b)$$

$$T_{D,\max}(E, P_R, P_R^W, L) < T_{\text{therm. degrad.}} \text{ (60°C)} \qquad (12c)$$

Constraints (12a), (12b), and (12c) are to be satisfied at any time in order to ensure a satisfactory operation without corona discharge, melt back of the frozen material, and thermal degradation of the dry product. In the four-dimensional space of the process variables (E, P_R, P_R^W, L) this domain corresponds to the innermost volume enclosed by the coordinate frame planes and the three limiting hyper-surfaces defined by the tight constraints. It should be noted that the initial sample temperature and the ambient vacuum temperature are not accounted for as they were found not to be significant parameters.

The feasible operation domain is illustrated in Figure 9 where the limiting surface defined by the tight constraint

$$T_{F,\max}(E, P_R, P_R^W, 1.27) = -1.5°\text{C} \qquad (13)$$

has been calculated for a one-inch thick symmetric slab ($L = 1/2$ in. or 1.27 cm). The maximum electric field strength, allowable before melting of the frozen material occurs, was determined at various pressures P_R and P_R^W. The inner volume between the limiting surface, the first bisector plant $P_R = P_R^W$, and the planes $E = 0$ and $P_R^W = 0$ represents the feasible operation domain with respect to constraint (12b). In other words, if the operating conditions correspond to a point inside this volume, no melt back will occur at any time during the process. On the contrary, if an operation point is taken outside this domain, it will result in melting of the frozen material in the course of drying. However, the upper limit of 60°C may well be exceeded as Constraint (12c) is not considered. The entire feasible operation domain could be determined for a given practical system by a similar study conducted at various thicknesses. Constraints (12a) and (12c) should be included in order to ensure that no thermal degradation of the dried product would occur due to excessive heating of the dried product layer and that there would be no corona discharge in the microwave applicator.

Figure 9 shows that an increase of the ambient pressure or partial pressure of water vapor required that the electric field be reduced substantially in order to keep the sample frozen. This is due to the fact that the mass transfer resistance is increased or that the driving force is lowered which results in a higher temperature of the front and the ice core. Thus, considering the fact that the drying time decreases as the electric field is increased, Figure 9 indicates that an optimum operation would be at pressures P_R and P_R^W as low as possible, as a higher field strength could be applied without melt back. Figure 9 also shows that as P_R and P_R^W decrease and approach 0.2 mmHg, little gain is made on the maximum allowable field strength. In fact, at low pressures the vapor flow regime in the dry layer is mostly Knudsen diffusion for which the diffusivity is independent of the pressure. As far as the melting constraint is concerned, pressures below 50 μHg would represent a cost increase for the vacuum system but no significant gain in reducing the drying time. However, lower pressures may permit a higher operating electric field strength and thus further reduce the drying time as the field breakdown value in the vacuum increases (Gould and Kenyon, 1971).

Effects of the Process Variables on the Drying Time

As one may have expected, the drying time is a strong function of the electric field strength. The drying time has been plotted in Figure 10 vs. the reciprocal of the square of the electric field at various pressures and a vapor partial pressure of 0.075 mmHg. It can easily be seen that the drying time varies linearly with $1/E^2$. In other words, the drying time is inversely proportional to the microwave power input. It is found also that an increase of the total

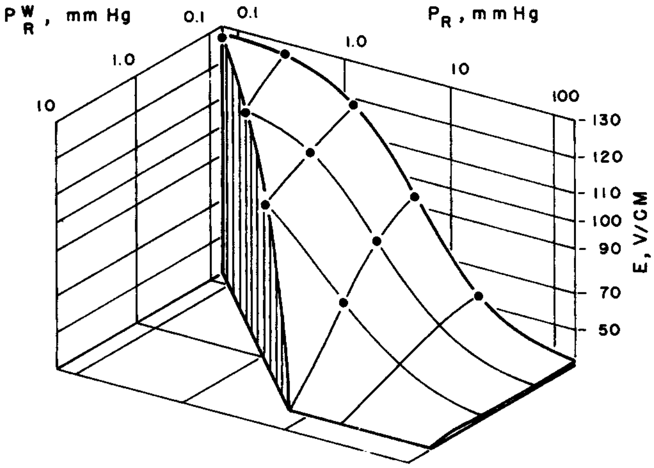

Fig. 9. Limiting surface for the feasible operation domain corresponding to the no melting constraint ($L = 1.27$ cm).

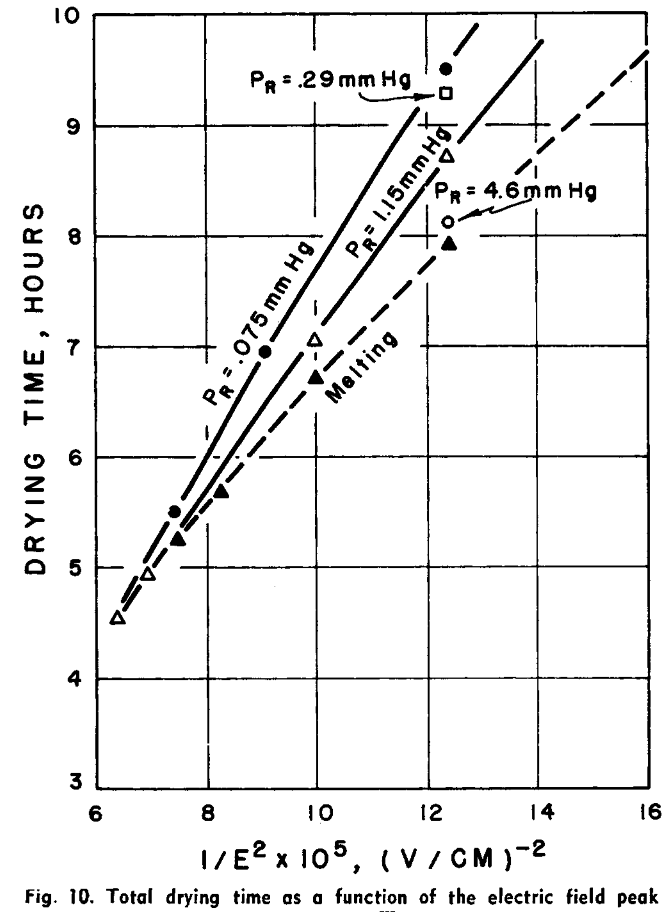

Fig. 10. Total drying time as a function of the electric field peak strength. $L = 1.27$ cm, $P_R^W = 0.075$ mmHg.

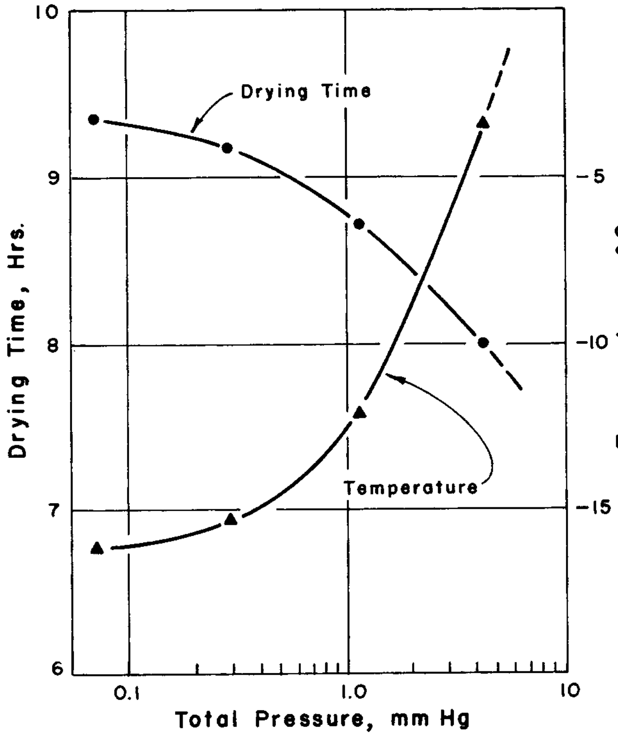

Fig. 11. Effects of the total ambient pressure upon the drying time and the maximum temperature reached by the frozen core. $E = 90$ V/cm, $P_R^W = 0.075$ mmHg, $L = 1.27$ cm.

pressure decreases the drying time, as shown on Figure 11. This is due to the higher dissipation coefficient (mainly in the frozen region) due to the increase in temperature in the sample (Figure 11) because of the greater mass transfer resistance in the dry layer. The small variation of the drying time with total pressure in the vacuum chamber indicates that the process is essentially controlled by the heat supply rate. However, the mass transfer resistance has a significant effect on the drying time as it causes variations of the actual sample temperature and, thus, limits the microwave power input.

The variations of the total drying time with L in Figure 12 seem to be in contradiction with results reported by Hoover et al. (1966). They observed that experimental drying times were essentially independent of the thickness. The results shown in Figure 12 may be supported by an approximate calculation of the total drying time t_2 by neglecting the variations of the dissipation coefficient K with time and location and approximating the power consumed by the phase change Q_i by the microwave power Ω_T absorbed in the sample. It is found that

$$t_2 = t_1 + \frac{\rho\, \sigma\, \Delta H_s}{(K_F - K_D)E^2} \operatorname{Log}\left(1 + \frac{K_F - K_D}{K_D}\ \frac{X_1}{L}\right) \tag{14}$$

Equation (14) shows that when the sample thickness is reduced, the overall drying time t_2 decreases as the fraction of the product remaining to be dried (X_1/L) at the end of the startup period decreases. If the thickness is further reduced, t_2 eventually reaches t_1 as X_1/L goes to zero (all frozen material removed at the end of the startup period). The drying process then becomes only radiant heating for which the drying time goes to zero with the sample thickness L. These variations of t_2 are in agreement with those shown in Figure 12. The maximum of the curves at higher thicknesses in Figure 12 can be attributed to the temperature increase (mainly in the frozen core) due to the increase of the mass transfer resistance when the thickness of the dried layer is increased as discussed previously. The higher temperatures in the sample increase the dissipation coefficient in both the frozen and dried regions, which cause more microwave power to be absorbed by the sample and thus shortens the drying time. Figure 12 indicates that smaller slab thicknesses would enable one to use higher electric field strengths to shorten drastically the drying time without melting.

Optimal Operation

It has been mentioned earlier that, as far as the total pressure and the partial pressure of water vapor in the vacuum chamber are concerned an optimal operation would correspond to an operation under pressures as low as possible. Lower pressures give lower sample temperatures during drying and permit a higher microwave power input and thus shorten drying times. However, use of pressures below 50 μHg to prevent melt back is impractical as previously discussed.

On the other hand, Figure 13 shows that, for a given electric field strength, the optimal thickness yielding the highest output of dried product is the largest thickness without occurrence of melting of the frozen material or overheating of the dried product. Figure 13 shows indeed that, under the assumptions made here, overheating of the dried product could occur earlier than melting of the frozen core. However, it should be mentioned that the numerical value of the diffusivity used in the calculations may have been overestimated in this case. This would mean that the actual temperatures in the sample are indeed somewhat higher than those computed here and thus melting may occur earlier than predicted. The negative slope of the overheating limiting curve in Figure 13 indicates that use of smaller thicknesses would increase the freeze-dryer output as higher field strengths are made possible.

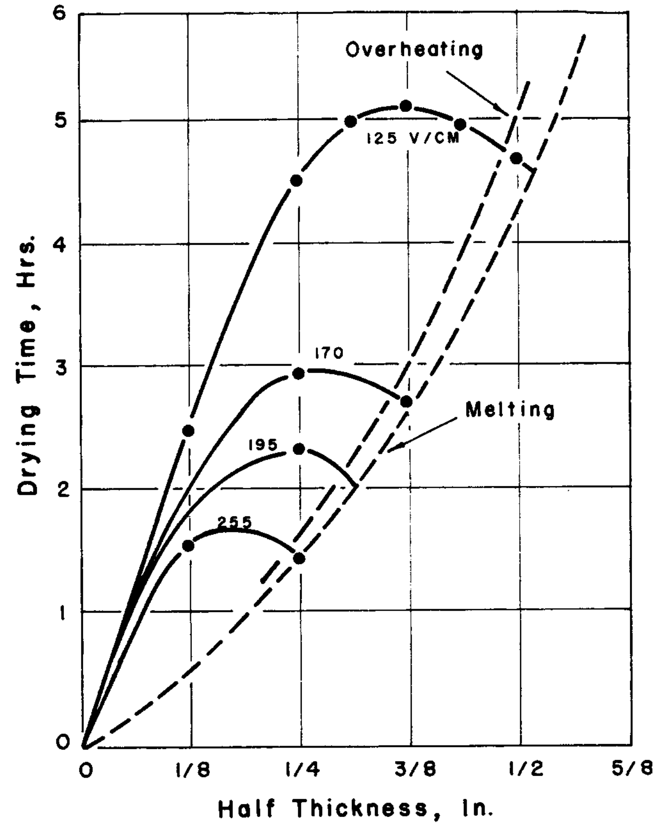

Fig. 12. Effects of the sample thickness on the total drying time for various electric field peak strengths. $P_R = P_R^W = 0.075$ mmHg.

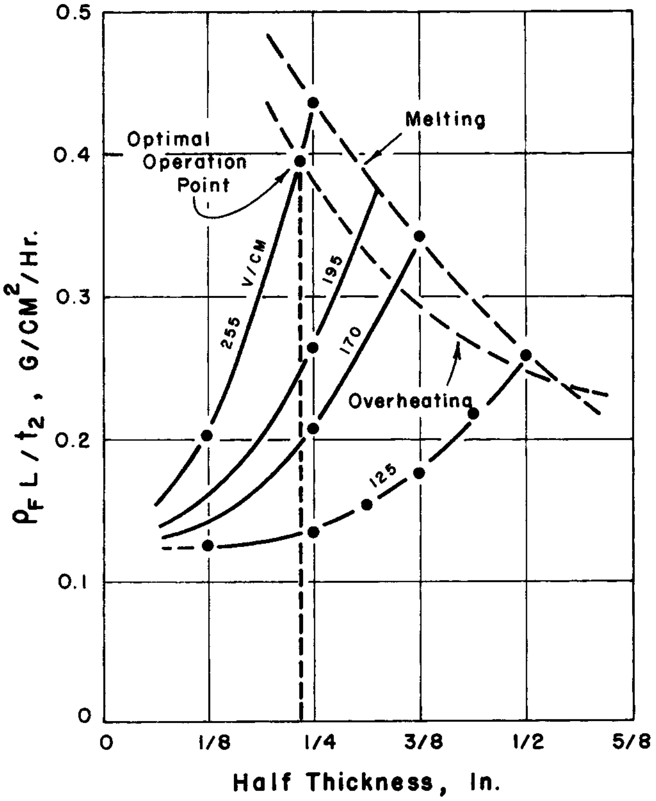

Fig. 13. Effects of the sample size on the output of the microwave freeze dryer for various electric field peak strengths. $P_R = P_R{}^W = 0.075$ mmHg.

However, as the electric field strength is increased, a corona discharge may develop in the microwave applicator, reducing drastically the power conversion efficiency and possibly inducing burns of the products. Thus, the optimal thickness yielding the maximum freeze-dryer output is that which would correspond to an operation near corona and overheating occurrence (or melting). For instance, if a corona discharge was to develop slightly about 255 V/cm which seems to be a reasonable assumption for the operating pressure and the microwave applicator used (Gould and Kenyon, 1971) the optimal thickness would correspond to the optimal operation point shown in Figure 13. It is important to note that the previous discussion had assumed an operation under low pressures ($P_R = P_R{}^W = 0.075$ mmHg) in order to ensure the lowest possible temperatures in the frozen region and the dry layer. Under these conditions and the assumptions made, if corona were to occur beyond 255 V/cm, a drying time as short as an hour and one half (including the 30 min. startup period), should be possible for a 1/2-in. slab. This would result in a maximum freeze-dryer throughput of approximately 0.8 g of frozen product per hour per square centimeter of surface area for a symmetric slab.

ACKNOWLEDGMENT

This research is supported by the U.S. Army Natick Laboratories through Grant DAAG 17-71-G-01. Use of the facilities of the Worcester Area College Computation Center is gratefully acknowledged.

NOTATION

C = concentration of water vapor in the pores, g/cm^3
C_D = specific heat of the dried material, cal/g-°K
C_F = specific heat of the frozen material, cal/g-°K
C_{pw} = specific heat of the water vapor, cal/g-°K
D = effective diffusivity, cm^2/s
D^0 = bulk diffusivity at 1 atm, cm^2/s
D_K = Knudsen diffusivity, cm^2/s
E = electric field peak strength in the vacuum, V/cm
E_B = electric field peak strength at breakdown, V/cm
f = microwave frequency, Hz
h = heat transfer coefficient, cal/s-cm^2-°K
ΔH_s = enthalpy of sublimation, cal/g
k = effective thermal conductivity, cal/s-cm-°K
K = dissipation coefficient defined by Equation (4b), cal/s-cm^3-(V/cm^2)
L = sample half thickness (symmetric slab), cm
P = total pressure, mmHg
P^w = partial pressure of water vapor, mmHg
Q = heat flux, cal/s-cm^2
S = normalized interface position
t = process time, s
T = temperature, °K
W = effective mass flux of water vapor, g/s-cm^2
x = space-coordinate, cm
x_w = initial moisture content of beef sample (wet basis)
x_f = initial fat content of beef sample (wet basis)
X = interface position, cm

Greek Letters

ϵ_0 = dielectric constant in vacuum (CGS)
ϵ' = relative dielectric constant
ϵ'' = relative loss factor
ρ = density of ice, g/cm^3
ρ_D = density of the dried material, g/cm^3
ρ_F = density of the frozen material, g/cm^3
σ = porosity (void fraction)
ω = density of microwave power absorbed, cal/s-cm^3
Ω = microwave power absorbed per unit area, cal/s-cm^2

Superscripts and Subscripts

0 = initial value; before the microwave power is turned on
1 = starting value; immediately before the microwave power is turned on
2 = final value; as the frozen core disappears
D = in the dry layer
F = in the frozen region
i = at the interface
R = in the vacuum (room)
S = at the outer surface
max. = maximum value

LITERATURE CITED

Awberry, J. H., and E. Griffiths, "Thermal Properties of Meat," *J. Soc. Chem. Ind.*, **52**, 326 (1933).

Bralsford, R., "Freeze-Drying of Beef," *J. Food Technol.*, **2**, 339 (1967).

Copson, D. A., "Microwave Sublimation of Foods," *Food Technol.*, **12**, 270 (1958).

———., *Microwave Heating in Freeze-Drying, Electronic Ovens and Other Applications,* Avi Publ. Co., Westport, Conn. (1962).

Dyer, D. F., and J. E. Sunderland, "Bulk and Diffusional Transport in the Region between Molecular Flow and Viscous Flow," *Intern. J. Heat Mass Transfer,* 9(6), 519 (1966).

Fox, E. C., and W. J. Thompson, "Coupled Heat and Mass Transport in Unsteady Sublimation Drying," *AIChE J.*, **18**, 792 (1972).

Gouigo, E. I., L. S. Malkov, and E. I. Kaukhcheshvili, "Certaines Particularites du Transfert de Chaleur et de Masse au Cours de la Lyophilisation de Produits Poreux dans un Champ Ultra Haute Frequence," Inst. Intern. du Froid, Commission X, Lausanne, Switz. (1969).

Gould, J. W., and F. M. Kenyon, "Gas Discharge and Electric Field Strength in Microwave Freeze-Drying," *J. Microwave Power*, 6(2), 151 (1971).
Harper, J. C., "Transport Properties of Gases in Porous Media at Reduced Pressures with Reference to Freeze-Drying," *AIChE J.*, 8, 298 (1962).
Hill, J. E., and J. E. Sunderland, "Sublimation in Dehydration in the Continuum, Transient and Free-Molecule Flow Regimes," *Intern. J. Heat Mass Transfer*, 14, 625 (1971).
Hill, J. E., J. D. Leitman, and J. E. Sunderland, "Thermal Conductivity of Various Meats," *Food Technol.*, 21, 1143 (1967).
Hohner, G. A., *An Analysis of Heat and Mass Transfer in Atmospheric Freeze-Drying*, Ph.D. thesis, Mich. St. Univ., East Lansing (1970).
Hoover, M. W., A. Markantonatos, and W. N. Parker, "UHF Dielectric Heating in Experimental Acceleration of Freeze-Drying of Foods," *Food Technol.*, 20, 103 (1966).
———., "Engineering Aspects of Using UHF Dielectric Heating to Accelerate the Freeze-Drying of Foods," *ibid.*, 107 (1966).
Jackson, S., S. L. Rickter, and C. O. Chichester, "Freeze-Drying of Fruit," *Food Technol.*, 11, 468 (1957).
Kan, B., and R. A. Yeaton, "Improving Freeze-Drying Process Efficiency through Improved Vapor Removal and In-Process Moisture Determination," QM Contract Report, DA 19-129-QM-1546 (1961).
King, C. J., *Freeze-Drying of Foods*, CRC Monoscience Series, (1971).
Lentz, C. P., "Thermal Conductivity of Meats, Fats, Gelatin Gels and Ice," *Food Technol.*, 15, 243 (1961).
Ma, Y. H., and P. Peltre, "Mathematical Simulation of a Freeze-Drying Process Using Microwave Energy," AIChE Symp. Ser. *No. 132*, 69, 47 (1973).
———., "Freeze Dehydration by Microwave Energy: Part II. Experimental Investigation," *AIChE J.*, 21, 344 (1975).
Miller, H. L., and J. E. Sunderland, "Thermal Conductivity of Beef," *Food Technol.*, 17, 124 (1963).
Peltre, P., *Freeze-Dehydration by Microwave Energy*, Ph.D. thesis, Worcester Polytechnic Inst. Mass. (1974).
Rey, L., *Aspects Théoriques et Industriels de la Lyophilisation*, Herman, Paris (1964).
Sandall, C. C., C. J. King, and C. R. Wilke, "The Relationship Between Transport Properties and Rates of Freeze-Drying of Poultry Meat," *AIChE J.*, 13, 428 (1967).
Therlkeld, J. L., *Thermal Environmental Engineering*, Prentice Hall, Englewood Cliffs, N. J. (1962).
Wakao, N., S. Otani, and J. M. Smith, "Significance of Pressure Gradients in Porous Materials: Part 1., Diffusion and Flow in Fine Capillaries: Part 2., Diffusion and Flow in Porous Catalysts," *AIChE J.*, 11, 435 (1965).

Manuscript received August 21, 1974; revision received December 26, 1974, and accepted January 2, 1975.

Freeze Dehydration by Microwave Energy:

Part II. Experimental Study

Experimental drying curves have been obtained for the freeze-dehydration of beef meat with microwave energy at 2450 MHz. In particular, experiments conducted with slabs of raw beef meat approximately 1.5 cm thick show that total drying times of less than 6 hr. can be obtained. Further drying time reductions are possible if microwave heating and freezing techniques are improved. Samples can be dried slightly faster at a higher pressure (for example, 1 mmHg) than at a lower pressure (for example, 0.2 mmHg) for the same microwave power input. However, melt back and vaporization occur if the pressure or the microwave power input is too high.

Comparison of the experimental drying curves with those predicted by the theory shows a reasonable agreement which, at least in part, verifies the validity of the previously derived mathematical model.

YI HUA MA
and
PHILIPPE R. PELTRE

Department of Chemical Engineering
Worcester Polytechnic Institute
Worcester, Massachusetts 01609

SCOPE

Although freeze drying is normally considered to be a slow process, the acceleration of the process can be achieved by the application of volumetric heating (for example, microwave energy) as previously demonstrated (Jackson et al., 1957; Copson, 1958). Previous work concentrated mostly in demonstrating the feasibility of microwave energy for freeze drying. A detailed theoretical investigation with a verification by an experimental study is lacking.

The present work employed an experimental multimode cavity to investigate the freeze-dehydration of beef meat at a microwave frequency of 2450 MHz. Utilization of a specially designed continuous weighing system provided a means of investigating the effects of the microwave power input and the total pressure of the vacuum upon the drying rate. Melt back of the sample at high microwave power input and at high pressure in the vacuum chamber was observed. Comparison of the experimental drying curve with those predicted by the model previously developed by the authors (Peltre, 1974; Ma and Peltre, 1975) showed a good agreement between the experimental and theoretical results.

Correspondence concerning this paper should be addressed to Y. H. Ma. P. R. Peltre is with the U.S. Army Natick Laboratories, Natick, Massachusetts.